Paper No.
PP6

Corrosion behaviour of nanophase modified fly ash concrete reinforced with TMT rebar for seawater applications

U. Sudha

[1]Centre for Nanoscience and Nanotechnology, Sathyabama University,
Chennai-600119, India
Sudha21190@gmail.com

Vinita Vishwakarma[1], D.Ramachandran[1], Manu Harilal[2], B. Anandkumar[2], R. P. George[2]*and U. Kamachi Mudali[3]

[2]Corrosion Science and Technology Group, Indira Gandhi Centre for Atomic Research,
Kalpakkam-603 102, India

[3]Materials Chemistry and Metal Fuel Cycle Group, Indira Gandhi Centre for Atomic Research,
Kalpakkam- 603102

ABSTRACT

The corrosion of reinforced steel embedded in concrete structures is a universal threat to its integrity, finally leading to its failure. The steel reinforcement in concrete structures can be protected against corrosion using modification techniques. With the aim of increasing the durability and corrosion resistance property of concrete structures, supplementary cementitious materials and nanoparticles are being incorporated into the concrete. In the present work, four different concrete mixes were designed, fabricated and named as FA (fly ash concrete), FAT (fly ash with 2 wt% nano-titania), FAC (fly ash with 2 wt% nano-calcium carbonate) and FATC (fly ash with 1 wt% nano-titania and 1 wt% nano-calcium carbonate). All the specimens were reinforced with SAIL TMT steel rebar and tested under exposure to seawater for a period of 18 weeks. The corrosion parameters of the concrete with rebar was continuously monitored with techniques like Open Circuit Potential (OCP) monitoring and Linear Polarization Resistance (LPR) measurement. Test (RCPT). The detailed surface and phase analysis of the concrete specimens were carried out utilizing Scanning Electron Microscopy (SEM). Results confirmed that the incorporation of nanoparticles have greatly improved the corrosion resistance of the reinforced concrete specimens in comparison with fly ash concrete. The extent of degradation was observed to be the least in concrete specimen incorporated with nano-TiO_2 and nano-$CaCO_3$ (1:1 wt%) indicating its enhanced deterioration resistance

Keywords: flyash, nanophase modification, corrosion, TMT rebar

1.0 INTRODUCTION

The corrosion of reinforced steel embedded in concrete structures is a great quandary everywhere. The steel rebar generally subsists in a passive state and attributes to compose thin iron oxide layer on the steel surface which can be stable even in highly alkaline environment (pH 11-13) of concrete [1]. The corrosion process involves the apportionment of the protective passive layer which leads to an expansion in the cross-section of the reinforced steel due to the formation of high volume corrosion products [2]. The deterioration of steel rebar reduces the life expectancy of concrete structures and loss of structural stability. In marine structures, chloride induced assailment is the most mundane cause of corrosion [3]. The utilization of corrosion inhibitors and mineral admixtures may be a good alternative because of its easy application and lower cost to protect the passive layer ravagement due to corrosion [4-8]. Nowadays sundry types of corrosion inhibitors are utilized in concrete mix to for the concrete stability [9]. The efficacy of utilizing mineral admixtures like fly ash, slag and silica fume in concrete is well established [10-12]. Studies conducted with 10-40% fly ash replacement with cement, showed enhanced corrosion resistance compared to OPC concrete [13]. Substitution of fly ash with concrete up to 50% replacement showed drastic decrease in chloride permeability [14]. The addition of 20% fly ash showed lower corrosion resistivity compared to OPC concrete [15]. This work addresses the corrosion behavior of fly ash and nanophase modified fly ash concrete in sea water environment. The results are discussed in detail.

2.0 EXPERIMENTAL PROCEDURE

2.1 MATERIALS AND MIX DESIGN OF CONCRETE

Ordinary Portland cement (43 Grade) conforming to IS 8112-2013 and class-F Flyash (Ennore, Tamil Nadu) were used as cementitious materials for this study. The coarse aggregate with maximum size 20 mm and 12 mm in compliance with the requirements of IS 383 and river sand (river bed, Palar) with size of 4.75 mm was used as fine aggregate. Supaplast HP (SP-430, Fosroc Chemicals Ltd., Bangalore, India), a high range water reducer conforming to ASTM C-494 type G was used as admixture.

The commercial grade titanium dioxide (TiO_2), anatase (TTP, Kerala) and calcium carbonate ($CaCO_3$) (Arathanghi chemical, Tamil Nadu) purchased, had the initial size of 130-655 nm. The nanoparticles were ground using ball mill (SPEX 8000M-230 dual mixer mill, 230V/50 Hz). The final size of the ball milled $CaCO_3$ and TiO_2 nanoparticles were found to be in the range of 50-80 nm and 50-70 nm respectively.

Four types of concrete mix designated as FA (40% replacement of cement with flyash), FA replaced with 2% TiO_2 nanoparticles (FAT), FA with 2% $CaCO_3$ nanoparticles (FAC) and FA with 1 % TiO_2 and 1 % $CaCO_3$ (FATC) were casted as per IS 8112:1989. All the specimens were casted as reinforced cylindrical concrete with two steel rods. All specimens were demolded after 24 h of casting and the specimens were cured for 28 days in fresh water.

2.2 ELECTROCHEMICAL STUDIES

Electrochemical measurements on the concrete specimens were carried out with an ACM Galvo Gill electrochemical workstation (Gill 12). The typical three electrode system was used for the measurements where, a saturated Ag/AgCl electrode was the reference electrode and the working and counter electrodes were the TMT rebars used in the study. The concrete specimens were immersed in seawater for a period of 4 months. The corrosion behaviour of the rebars was perpetually monitored using the techniques like Open Circuit Potential (OCP) and Linear Polarization Resistance (LPR). The OCP measurement was carried out for a period of 1 hour followed by determination of its resistance upon linear polarization in the range of ± 25 mV at the scan rate of 10mv/min.

2.3 SURFACE AND PHASE ANALYSIS

The concrete specimens were broken after the exposure period. The surface of the steel rebar and the concrete surface were examined by Scanning Electron Microscopy (SEM). The detailed phase analysis of the concrete specimens was carried out by X-ray Diffraction (XRD) technique after pulverizing the samples.

3.0 RESULTS

3.1 OPEN CIRCUIT POTENTIAL MEASUREMENTS

Figure 1 represents the Open Circuit Potential (OCP) values of the reinforcing steel bar embedded in four types of concrete specimens exposed in seawater for a period of over four months measured against Ag/AgCl reference electrode. From the figure, it can be clearly inferred that initially all the specimens had a negative potential value indicating the active condition of the embedded steel reinforcement. Among all the mixes, FATC had the maximum OCP value of over -200 mv and FAT had the least value. However, it can be seen that even after complete exposure in seawater for 4 months, the OCP values of the FATC concrete specimens still remained constant whereas there was a large increase in the OCP values of FAT concrete specimens pointing out the active condition of the rebar. There was a slight marginal increase in the OCP values of FA specimens. Thus, it can be concluded that nanophase modification of the flyash concrete specimens have improved the corrosion resistance of the rebars by maintaining a passive state.

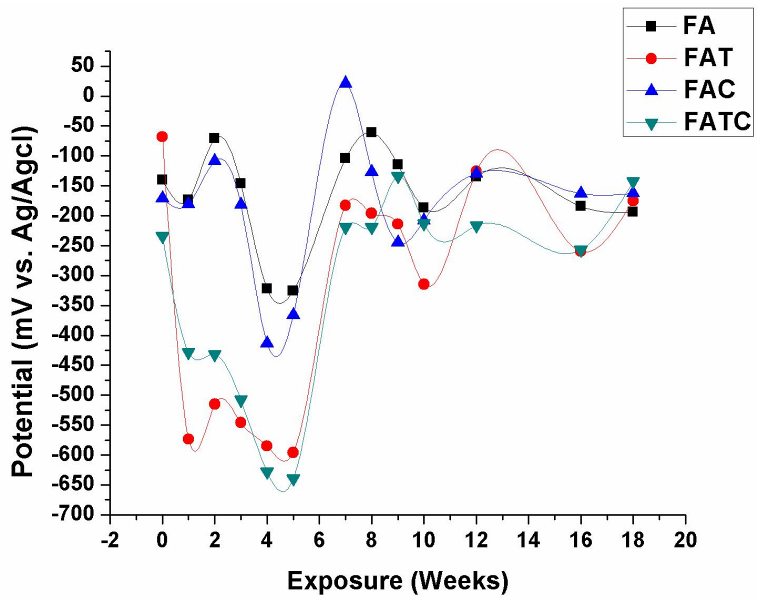

Figure 1: OCP of concrete specimens exposed in seawater

3.2 LINEAR POLARIZATION RESISTANCE

The data collected from Linear Polarization Resistance (LPR) measurement are tabulated in table 4 below. The LPR measurement has been carried out on all the four concrete mixes over a period of 4 months. The results reveal that the FATC concrete specimens have shown high polarization resistance (R_p) values compared to all the other mixes. Both FAC and FATC specimens exhibited a similar trend in the R_p values. However, the addition of nano-titania alone couldn't improve the corrosion resistance of the embedded rebar in FAT mix as is evident from the comparatively lower R_p value for this type of concrete mix. The trends in the I_{corr} values confirm the above statements. A high value of I_{corr} indicates high levels of corrosion. Both FAC and FATC specimens had least I_{corr} value proving their high resistance against the corrosion of the reinforcement. FAT had a marginal rise in I_{corr} value indicating comparatively enhanced levels of reinforcement corrosion.

Thus, incorporation of nano-TiO_2 and nano-$CaCO_3$ in equal proportions to flyash concrete has greatly amended its resistance against the corrosion of the steel reinforcement.

Table 1. Potentiostatic polarization parameters of sea water exposed concrete specimens

Duration of exposure (Weeks)	FA		FAT		FAC		FATC	
	R_p (Ω cm^2)	I_{corr} (mA/cm^2)	R_p (Ω cm^2)	I_{corr} (mA/cm^2)	R_p (Ω cm^2)	I_{corr} (mA/cm^2)	R_p (Ω cm^2)	I_{corr} (mA/cm^2)
0th Day	1662.50	0.007	2468.20	0.005	1912.70	0.006	1190.30	0.010
1	1583.20	0.008	626.85	0.019	1725.50	0.007	957.01	0.013
2	1681.50	0.007	623.59	0.019	2215.50	0.005	889.19	0.014
3	2307.30	0.005	832.31	0.014	2980.70	0.004	994.83	0.012
4	912.28	0.013	616.40	0.020	1023.00	0.012	520.67	0.023
5	923.20	0.013	572.14	0.021	1215.70	0.010	571.16	0.021
7	1338.90	0.009	550.60	0.022	1256.90	0.010	563.91	0.021
8	640.78	0.019	439.46	0.027	648.45	0.019	517.64	0.023
9	618.50	0.019	465.12	0.026	690.67	0.017	565.78	0.021
10	578.59	0.021	510.41	0.024	1640.00	0.007	886.65	0.014
12	377.06	0.032	468.14	0.026	506.72	0.024	951.89	0.013
16	453.33	0.027	283.47	0.042	688.06	0.018	592.53	0.020
18	518.63	0.023	412.06	0.029	612.93	0.020	617.03	0.020

Figure 2 represents a schematic diagram of the trends exhibited by different concrete mixes when subjected to linear polarization. It can be seen that the initial corrosion resistance offered by FAT specimen was the highest, which showed a continuous decrease when exposed in seawater. But, FAC and FATC specimens displayed comparatively higher levels of resistance against degradation in seawater. Thus, FATC can be recommended for applications in marine atmosphere due to this enhanced durability characteristics.

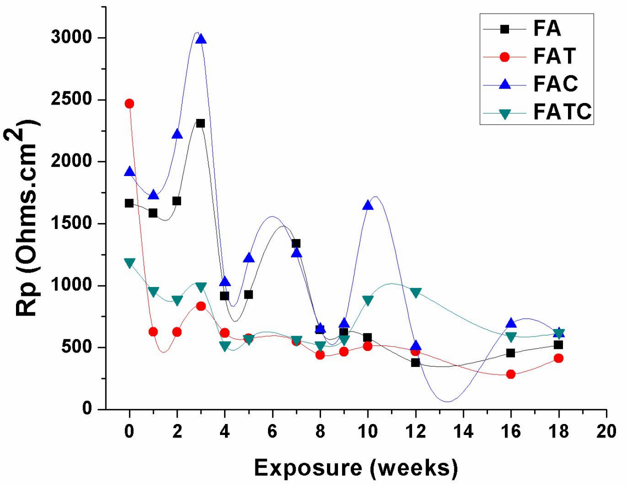

Figure 2: R_p values of concrete specimens exposed in seawater

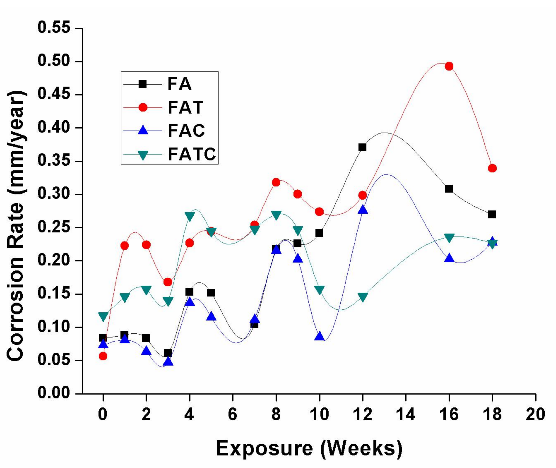

Figure 3: Corrosion rate of concrete specimens exposed in seawater

3.3 DETERMINATION OF CORROSION RATES

The corrosion rates of the four different types of concrete mixes were determined according to ASTM G102 – 89. Figure 3 schematically represents the trend observed in the corrosion rate of the reinforcing steel rebars with exposure in seawater for over four months. Among various types of concrete specimens, FATC and FAC showed least rates of degradation when exposed in a marine environment. However, FA had a tiny increase in the rate and FAT had a comparatively marginal increase in the corrosion rates. Table 2 represents the detailed data collected over the exposure period on all the various specimens. Thus, addition of nano-TiO_2 and nano-$CaCO_3$ to flyash concrete seems to a highly potential way of increasing its resistance against degradation.

Table 2. Corrosion rate of sea water exposed concrete specimens

Duration of exposure (week)	Specimen type			
	Corrosion rate (mmpy)			
	FA	FAT	FAC	FATC
0th Day	0.084	0.057	0.073	0.117
1	0.088	0.223	0.081	0.146
2	0.083	0.224	0.063	0.157
3	0.061	0.168	0.047	0.140
4	0.153	0.227	0.137	0.268
5	0.151	0.244	0.115	0.245
7	0.104	0.254	0.111	0.248
8	0.218	0.318	0.215	0.270
9	0.226	0.300	0.202	0.247
10	0.241	0.274	0.085	0.158
12	0.371	0.298	0.276	0.147
16	0.308	0.493	0.203	0.236
18	0.269	0.339	0.228	0.226

3.4 SURFACE AND PHASE ANALYSIS

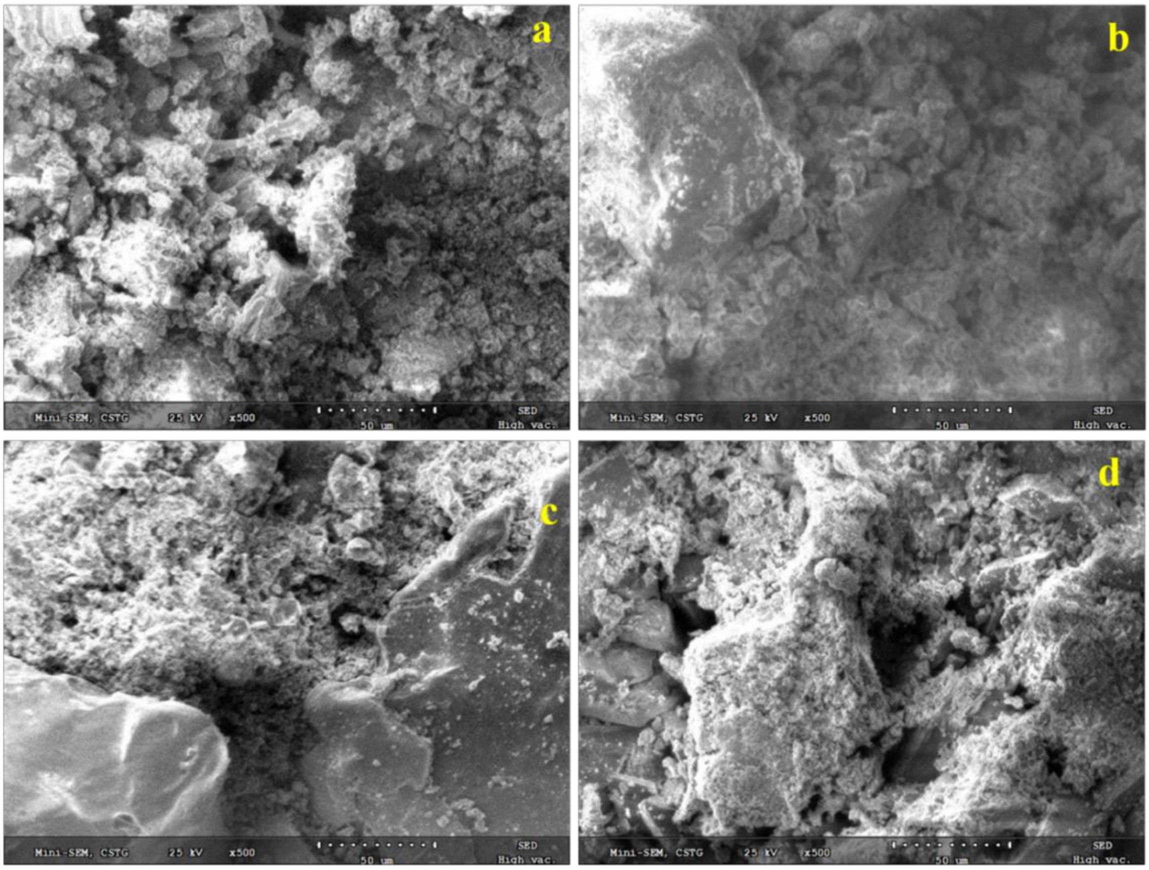

Figure 4: Unexposed concrete specimens (a) FA (b) FAT (c) FAC (d) FATC

Figure 4 illustrates the SEM images of 28 days cured concrete specimens which does not showed significant differences among four different mixes. Before exposure to the sea water, the specimens showed usual concrete constituents of calcium, silica and other hydration products. The integrity of the different mixes of concrete specimens remains same. However, after exposure to the sea water, huge difference was observed among all the specimens (Figure 5). The inset image of (a) FA concrete showed cracks which indicating severe degradation. The SEM image of (b) FAT concrete surface, showed the formation of C-S-H rocks which was confirmed by EDS. However, due to the non-uniformly formed hydration products, there were some pits and voids were observed. The SEM image of (c) FAC concrete specimen surface showed very less hydration products with some craters on the surface. The SEM image of FATC concrete showed deadlocked formation of C-S-H gel and other hydration products which reduced the pore structure of the concrete thereby the penetration of aggressive chemicals also reduced which indicating least degradation on FATC concrete surfaces.

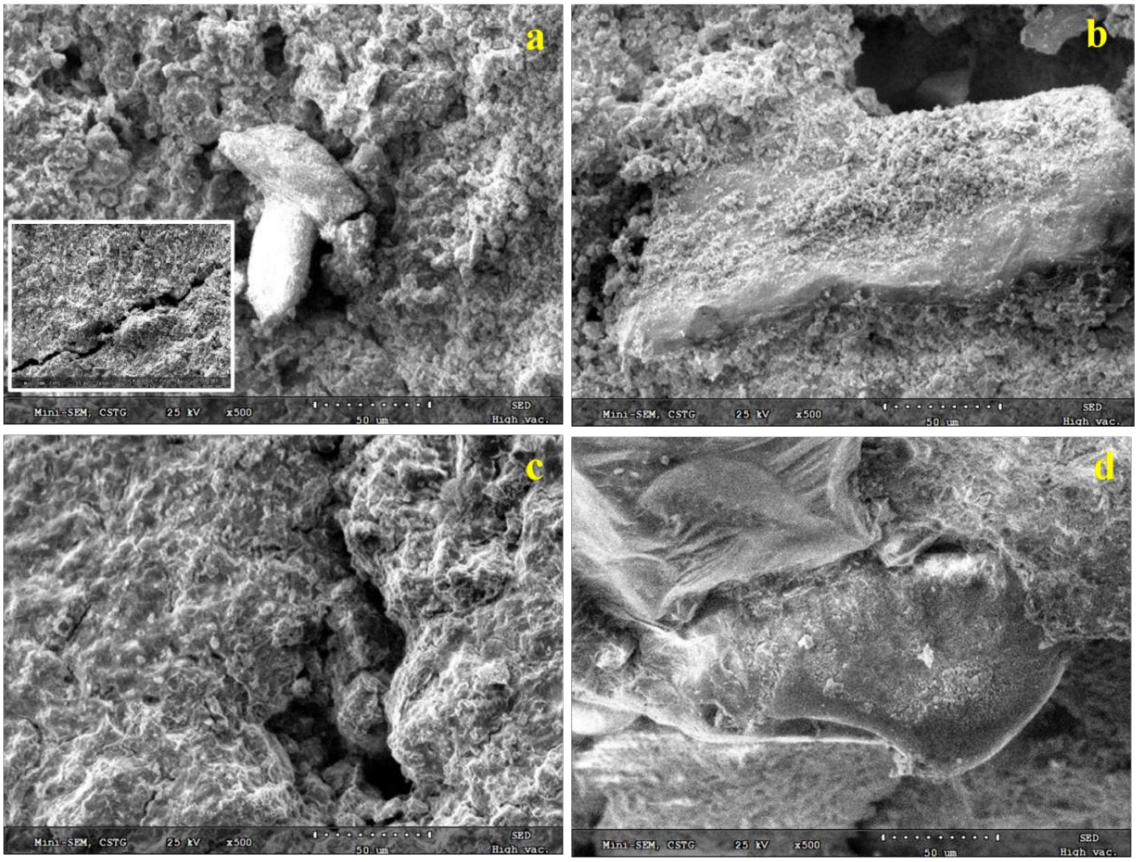

Figure 5: 4m sea water exposed concrete specimens (a) FA (b) FAT (c) FAC (d) FATC

4.0 CONCLUSIONS

ACKNOWLEDGMENTS (First level heading, Capital, Arial, 12, Bold)

Financial support from Board of Research in Nuclear Sciences (BRNS), Mumbai (2013/36/33-BRNS/2355 dated 26 November, 2013) is greatly acknowledged. The authors would also like to thank Dr Jeppiaar, Chancellor Sathyabama University, Chennai and Director, IGCAR, Kalpakkam for guidance, encouragement and motivation.

REFERENCES

[1] P. Garces, P. Saura, A. Mendez, E. Zornoza and C. Andrade: Effect of nitrite in corrosion of reinforcing steel in neutral and acid solutions simulating the electrolytic environments of micropores of concrete in the propagation period, Corrosion science, 2008, 50, 498–509.

[2] H.W. Song, V. Saraswathy, S. Muralidharan, C.H. Lee and K. Thangavel, Corrosion performance of steel in composite concrete system admixed with chloride and various alkaline nitrites, Corrosion Engineering, Science and Technology, 2009, Vol 44 No. 6

[3] T. A. Soylev, C. McNally and M. G. Richardson, Effectiveness of amino alcohol-based surface-applied corrosion inhibitors in chloride-contaminated concrete, Cement and concrete research, 2007, 37, 972–977.

[4] S. Qian and D. Cusson: Cem. Concr. Com., 2004, 26, 217–233.

[5] C. L. Page, V. T. Ngala and M. M. Page: Mag. Concr. Res., 2000, 52, 25–37.

[6] G. Trabanelli, C. Monticelli, V. Grassi and A. Frignani: Cem. Concr. Res., 2005, 35, 1804–1813.

[7] H. Saricimen, M. Mohammad, A. Quddus,M. Shameem and M. S. Barry: Cem. Concr. Com., 2002, 24, 89–100.

[8] V. T. Ngala, C. L. Page and M. M. Page: Corros. Sci., 2003, 45, 1523–1537

[9] D. M. Bastidas, A. Cobo, E. Otero and J. A. Gonzalez: Corrosion science engineering and technology., 2008, 43, 248–255. Electrochemical rehabilitation methods for reinforced concrete structures: advantages and pitfalls.

[10] V. Saraswathy and H. W. Song: Build. Environ. 2007, 42, 464–472.

[11] J. S. Reou and K. Y. Ann: Mater. Chem. Phys., 2008, 109, 526–533.

[12] K. Y. Ann, H. S. Jung, H. S. Kim, S. S. Kim and H. Y. Moon: Cem. Concr. Res., 2006, 36, 530–535

[13] Velu Saraswathy, Ha-Won Song, Electrochemical studies on the corrosion performance of steel embedded in activated fly ash blended concrete, Electrochimica Acta, Vol. 51, 4601-4611

[14] Tarun R. Naik, Shiw S. Singh, Permeability Of Concrete Containing Large Amounts Of Fly Ash, Cement and Concrete Research, Vol. 24, No. 5, pp. 913-922, 1994

[15] Xiaojian Gao, Yingzi Yang and Hongwei Deng, Electrochemical Changes of Pre-Corroded Steel Reinforced Concrete Due to Electrochemical Chloride Extraction, International Journal of Electrochemical Science, 6 (2011) 1797 - 1809